organic compounds

Intermolecular π-stacking and F···F interactions of fluorine-substituted meso-alkynylporphyrin

Yuta Marushima,[a] Yuri Uchiumi,[a] Kenichi Ogu[a] and Akiko Hori[a,b]*

[a]School of Science, Kitasato University, Kitasato 1-15-1, Minami-ku, Sagamihara, Kanagawa 252-0373, Japan, and [b]PRESTO, JST, Honcho 4-1-8, Kawaguchi, Saitama, Japan
Correspondence e-mail: hori@kitasato-u.ac.jp

Two C2-symmetric meso-alkynylporphyrins, namely 5,15-bis-[(4-butyl-2,3,5,6-tetrafluorophenyl)ethynyl]-10,20-dipropylporphyrin, $C_{50}H_{42}F_8N_4$, (I), and 5,15-bis[(4-butylphenyl)ethynyl]-10,20-dipropylporphyrin, $C_{50}H_{50}N_4$, (II), show remarkable π–π stacking that forms columns of porphyrin centers. The tetrafluorophenylene moieties in (I) show intermolecular interactions with each other through the F atoms, forming one-dimensional ribbons. No significant π–π interactions are observed in the plane of the phenylene and tetrafluorophenylene moieties in either (I) or (II). The molecules of both compounds lie about inversion centers.

Comment

Porphyrin assemblies allow chemists to create mechanical architectures and to understand biological systems (Drain et al., 2009; Beletskaya et al., 2009; Nakamura et al., 2007). For the past few decades, porphyrin derivatives with acetylene connections at the meso positions have found great utility as the motifs of self-assembling systems and electronic materials (Huang et al., 2006; Anderson et al., 1998). In particular, substitutions for the meso-alkynylporphyrins, while maintaining the coplanar molecule, are important in the development of intermolecular arrays in crystals and on surfaces (Kato et al., 2004). While many kinds of alkynyl, aryl and monohalogeno derivatives have been investigated, few examples of fluorine-substituted meso-alkynylporphyrins have been reported, such as those exhibiting mono-substitution by –F or –CF₃ groups (Kuo et al., 2007; Doerksen & Thakkar, 1999). We have been interested in the crystal packing of fully fluorinated aromatic compounds, because fluorine substitution controls the distance, direction and strength of the π-stacking based on the high electronegativity of the F atoms. The unique interactions induced by fluorine are demonstrated as arene–perfluoroarene (Williams, 1993; Hori et al., 2007, and refer-

ences therein), C—H···F (Thalladi et al., 1998) and anion···π (Quiñonero et al., 2002) interactions, amongst others. This prompted us to design the perfluorophenylene-attached meso-alkynylporphyrin (I) and to compare it with the nonfluorinated analogue (II), which hopefully will provide a good basis for understanding the intermolecular interactions and for designing further reactions of self-assembling motifs. The butyl and propyl groups were attached in order to increase the solubility of the compounds.

(I) X = F
(II) X = H
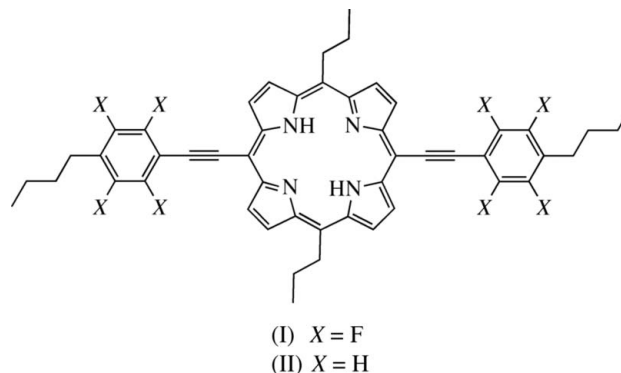
The two porphyrin derivatives were synthesized in two steps using the Linsey reaction (see Experimental). Crystallization by diffusion of MeOH into a CHCl₃ solution of the compounds yielded pure products. The UV–visible spectra of (I) and (II) in CH₂Cl₂ solution are very similar: both Soret bands are observed at 442 nm for (I) and (II), and the Q bands are observed at 603 and 698 nm for (I) and at 601 and 698 nm for (II). However, the diffuse reflection spectra of the powder samples with KBr of (I) and (II) are slightly but significantly different from the spectra in a CH₂Cl₂ solution. The peak tops of the broad bands are observed around 429–450, 626 and 716 nm for (I) and around 448, 618 and 710 nm for (II), which means that, except for the Soret band of (I), the bands are redshifted compared with a solution, as usual for the solid state. The small blue shift in the broad Soret band of (I) is attributed to the effects of intermolecular interactions.

Molecules of (I) and (II) lie across crystallographic inversion centers, with the porphyrin ring and the phenylene moieties almost coplanar (Fig. 1). However, the dihedral angle between them, viz. N1/N2/C1–C10 (12 porphyrin atoms) and C13–C18 (six phenylene atoms), in (I) is 10.72 (7)°, which is greater than that in (II) [2.29 (8)°]. The acetylene linkers in (I) are slightly sigmoidal in a plane perpendicular to the plane of the porphyrin moiety. Accordingly, the entire framework without H atoms, F atoms and aliphatic groups of the molecules of (I) is less flat than that of (II): the r.m.s. deviation of the aromatic atoms from their mean planes is 0.1076 Å in (I) and 0.0432 Å in (II). In (II), the sigmoidal form is also observed in the plane of the porphyrin moiety (Fig. 1). Bifurcated intramolecular N—H···N hydrogen bonds link amino atom N2 via H1 to imino atoms N1 and N1[i] (see Tables 1 and 2). The C5—C11, C11—C12 and C12—C13 distances around the acetylene linkage clearly indicate the localization of the triple bonds of the acetylene linkers in (I) and (II).
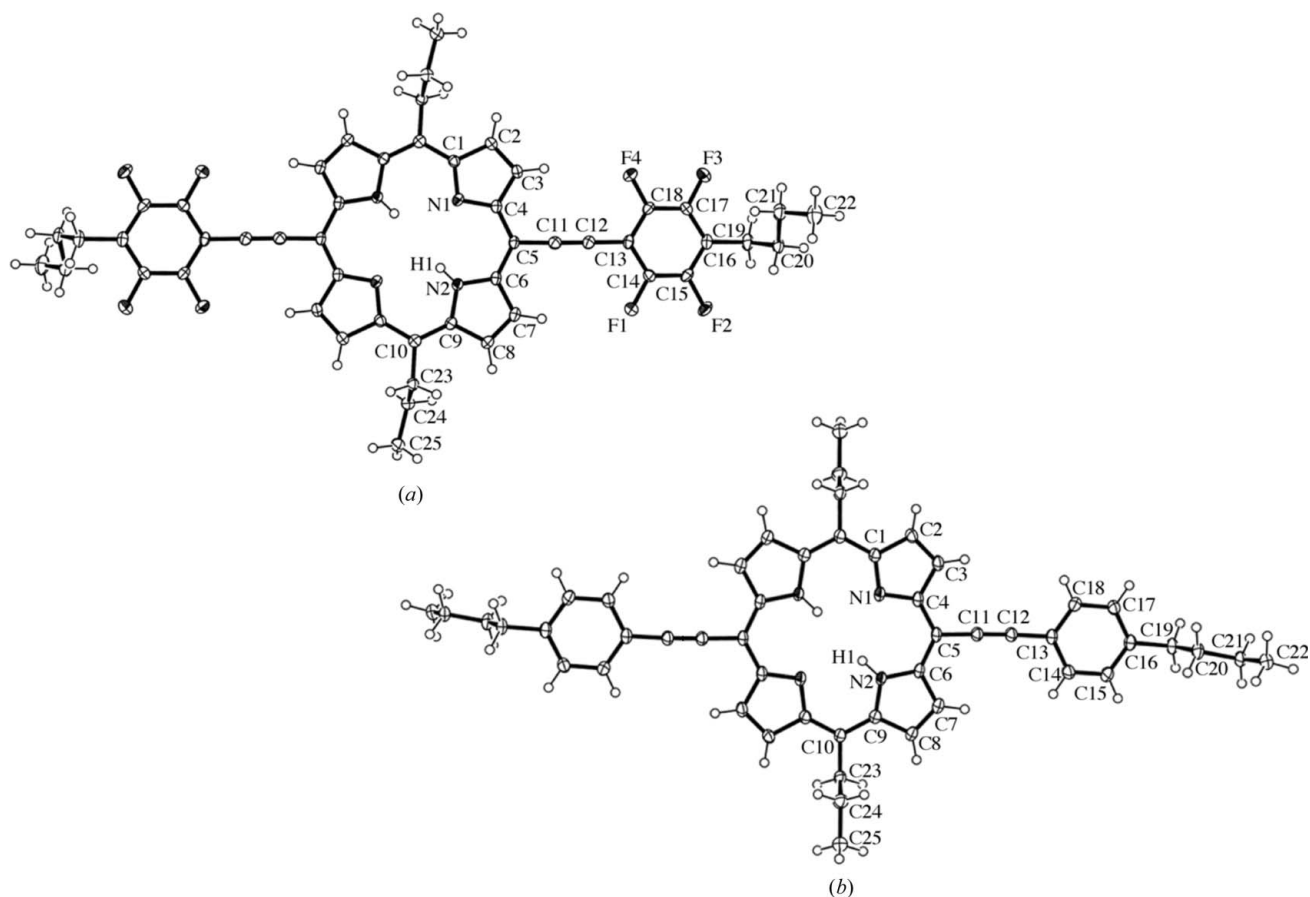
Figure 1
The molecular structures of (*a*) (I) and (*b*) (II) at 100 K, showing the atom-labeling schemes. Displacement ellipsoids are drawn at the 50% probability level.
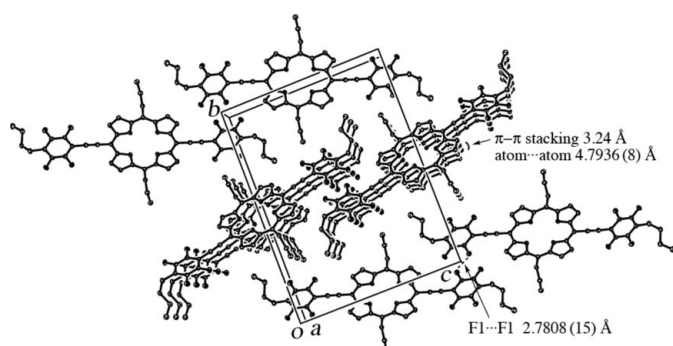

Figure 2
A view of part of the crystal structure of (I) along the *a* axis.

Figure 3
A view of part of the crystal structure of (II) along the *b* axis.

The crystal packing arrangements in (I) and (II) are shown in Figs. 2 and 3, respectively. In (I), the molecules are aligned in a flattened ribbon along the *c* axis, and an intermolecular F1···F1^{iii} interaction [symmetry code: (iii) $-x + 2, -y, -z$] of 2.7808 (15) Å is observed between the tetrafluorophenylene moieties. The ribbons are aligned parallel, with overlapping of half of the porphyrin moiety through intermolecular π–π stacking along the *a* axis, producing molecular columns. The corresponding intermolecular atom···atom distance of the molecules through the π–π stacking is 4.7936 (8) Å, the length of the *a* axis. The closest distance between the two pyrrole
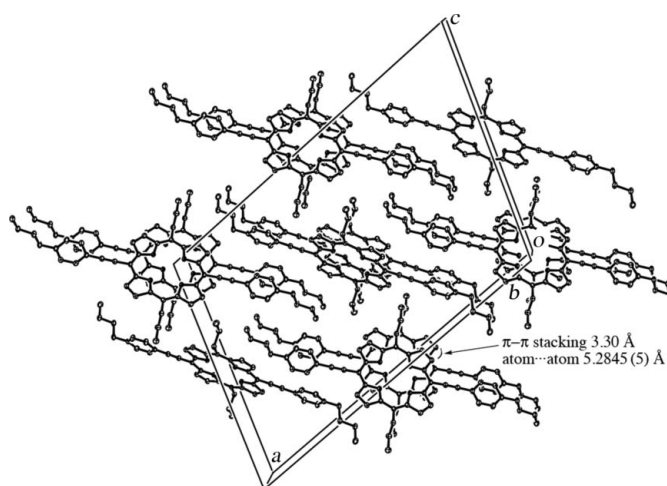
rings in the porphyrin center, CgA···CgB^{iv} [symmetry code: (iv) $x - 1, y, z$], is 3.7176 (12) Å, where CgA and CgB are the centroids of the five-membered N1/C1–C4 and N2/C6–C9 rings, respectively. The corresponding perpendicular distance from the ring centroids to the adjacent planes is 3.2399 (7) Å. In the column, the tetrafluorophenylene moieties are positioned close to each other and electrostatic π–π interactions

are dominant. The intermolecular distances between the two tetrafluorophenylene rings, $CgC\cdots CgC^{iv}$ and $CgC\cdots CgC^{v}$ [symmetry code: (v) $-x + 1$, $-y$, $-z$], are 4.7936 (8) and 5.1995 (13) Å, respectively, where CgC is the centroid of the tetrafluorophenylene ring C13–C18. The short $C-F\cdots CgC$ distances involving $C14-F1\cdots CgC^{vi}$ [symmetry code: (vi) $x + 1$, y, z] and $C17-F3\cdots CgC^{iv}$ are 3.3590 (13) and 3.3599 (13) Å, respectively. Finally, the columns are arranged in a zigzag fashion along the b axis and the dihedral angle between the two planes of porphyrins is 87.85 (14)°, with alternation of the aligned butyl and propyl chains.

In (II), the molecules also show π–π stacking to produce columns of molecules along the b axis. The corresponding intermolecular atom$\cdots$atom distance of the molecules through the π–π stacking is 5.2845 (5) Å, the length of the b axis and greater than that in (I). The closest intermolecular distance between the two pyrrole rings in the porphyrin center, $CgA\cdots CgB^{vii}$ [symmetry code: (vii) x, $y + 1$, z], is 3.5863 (10) Å and the perpendicular distance from the ring centroids to the adjacent planes is 3.3016 (7) Å. The lateral interaction along [102] between the columns is much weaker than that in (I). The phenylene ring is close to a butyl group and the acetylene linker of the other molecules, the short distances $H15\cdots H20A^{viii}$ [symmetry code: (viii) x, $y - 1$, z] and $C12\cdots H17^{ix}$ [symmetry code: (ix) $-x + \frac{1}{2}$, $y - \frac{1}{2}$, $-z + \frac{1}{2}$] being 2.31 and 2.83 Å, respectively. No remarkable π–π intermolecular interactions are observed for the phenylene moiety and the closest intermolecular distance between the two phenylene rings, $CgC\cdots CgC^{ix}$, is 4.9821 (10) Å. Along the c axis, the columns are arranged in a zigzag fashion and the inclination of the two planes of the porphyrins is 78.2 (13)°.

In conclusion, both $C2$-symmetric porphyrins show intermolecular π–π stacking between the porphyrin centers, and no unusual stackings were observed between the phenylene moieties in (I) and (II). On the other hand, the tetrafluorophenylene moieties in (I) interact with each other through $F\cdots F$ interactions to give planar porphyrin ribbons. Accordingly, the π–π overlap is more significant in (I) than in (II), which probably increases the H-aggregate character of porphyrin (I) to produce small blue shifts in the solid state.

Experimental

The porphyrins (I) and (II) were prepared in two steps using the general Linsey method (Anderson *et al.*, 1998). Typically, BF$_3$·Et$_2$O (0.40 mmol) was added to a solution of 4-butyl-2,3,5,6-tetrafluoro-phenylpropiolaldehyde (1.35 mmol) in CH$_2$Cl$_2$ (35 ml) and an excess amount of pyrrole (68 mmol) at 248 K. The reaction mixture was stirred for 30 min, the solution was washed with 10% aqueous NaOH and water, dried over MgSO$_4$, and purified by column chromatography to give *meso*-(4-butyl-2,3,5,6-tetrafluorophenylethynyl)di-pyrromethane in 86% yield. The product (1.17 mmol) was further reacted with *n*-butylaldehyde (1.17 mmol), BF$_3$·Et$_2$O (0.40 mmol) and 2,3-dichloro-5,6-dicyano-1,4-benzoquinone (DDQ) (1.17 mmol) under Linsey conditions to produce porphyrin (I) as a dark-blue powder in 6% yield. Porphyrin (I) was also obtained in the same yield from 4-butyl-2,3,5,6-tetrafluorophenylpropiolaldehyde and *meso*-propyldipyrromethane, which was prepared from *n*-butylaldehyde

and an excess amount of pyrrole, under the same conditions as the first method. Porphyrin (II) was prepared from 4-butylphenyl-propiolaldehyde and *meso*-propyldipyrromethane as a dark-blue powder in 1% yield.

For (I), UV–visible spectra in solution (CH$_2$Cl$_2$): 442 (ε = 410000 M^{-1} cm^{-1}), 603 (ε = 54400 M^{-1} cm^{-1}), 698 nm (ε = 37000 M^{-1} cm^{-1}); solid (KBr): 429–450, 626 and 716 nm. Elemental analysis calculated for C$_{50}$H$_{42}$F$_8$N$_4$ (%): C 70.58, H 4.98, N 6.58; found: C 70.23, H 4.98, N 6.53. For (II), UV–visible spectra in solution (CH$_2$Cl$_2$): 442 (ε = 413000 M^{-1} cm^{-1}), 601 (ε = 60000 M^{-1} cm^{-1}), 698 nm (ε = 48300 M^{-1} cm^{-1}); solid (KBr): 448, 618 and 710 nm. Elemental analysis calculated for C$_{50}$H$_{50}$N$_4$ (%): C 84.95, H 7.13, N 7.92; found: C 84.91, H 7.01, N 7.95.

Compound (I)

Crystal data

C$_{50}$H$_{42}$F$_8$N$_4$	$V = 1983.4$ (6) Å^3
$M_r = 850.88$	$Z = 2$
Monoclinic, $P2_1/n$	Mo $K\alpha$ radiation
$a = 4.7936$ (8) Å	$\mu = 0.11$ mm^{-1}
$b = 23.483$ (4) Å	$T = 100$ K
$c = 17.628$ (3) Å	$0.28 \times 0.08 \times 0.06$ mm
$\beta = 91.824$ (2)°	

Data collection

Bruker APEXII CCD diffractometer	10839 measured reflections
Absorption correction: empirical (using intensity measurements) (*SADABS*; Sheldrick, 1996)	4444 independent reflections
	3019 reflections with $I > 2\sigma(I)$
$T_{min} = 0.970$, $T_{max} = 0.993$	$R_{int} = 0.038$

Refinement

$R[F^2 > 2\sigma(F^2)] = 0.045$	H atoms treated by a mixture of independent and constrained refinement
$wR(F^2) = 0.108$	
$S = 1.01$	
4444 reflections	$\Delta\rho_{max} = 0.30$ e Å^{-3}
286 parameters	$\Delta\rho_{min} = -0.25$ e Å^{-3}

Compound (II)

Crystal data

C$_{50}$H$_{50}$N$_4$	$V = 3832.7$ (6) Å^3
$M_r = 706.94$	$Z = 4$
Monoclinic, $C2/c$	Mo $K\alpha$ radiation
$a = 33.613$ (3) Å	$\mu = 0.07$ mm^{-1}
$b = 5.2845$ (5) Å	$T = 100$ K
$c = 23.152$ (2) Å	$0.28 \times 0.14 \times 0.06$ mm
$\beta = 111.252$ (1)°	

Data collection

Bruker APEXII CCD diffractometer	10125 measured reflections
Absorption correction: empirical (using intensity measurements) (*SADABS*; Sheldrick, 1996)	4292 independent reflections
	3128 reflections with $I > 2\sigma(I)$
$T_{min} = 0.980$, $T_{max} = 0.996$	$R_{int} = 0.028$

Refinement

$R[F^2 > 2\sigma(F^2)] = 0.044$	H atoms treated by a mixture of independent and constrained refinement
$wR(F^2) = 0.110$	
$S = 1.03$	
4292 reflections	$\Delta\rho_{max} = 0.24$ e Å^{-3}
250 parameters	$\Delta\rho_{min} = -0.23$ e Å^{-3}

Table 1
Hydrogen-bond geometry (Å, °) for (I).

D—H$\cdots A$	D—H	H$\cdots A$	$D\cdots A$	D—H$\cdots A$
N2—H1$\cdots$N1	0.85 (3)	2.47 (3)	2.980 (2)	119 (2)
N2—H1$\cdots$N1^i	0.85 (3)	2.28 (3)	2.840 (2)	124 (3)

Symmetry code: (i) $-x + 2, -y, -z + 1$.

Table 2
Hydrogen-bond geometry (Å, °) for (II).

D—H$\cdots A$	D—H	H$\cdots A$	$D\cdots A$	D—H$\cdots A$
N2—H1$\cdots$N1^i	0.906 (18)	2.290 (18)	2.8586 (16)	120.5 (15)
N2—H1$\cdots$N1	0.906 (18)	2.425 (19)	2.9779 (17)	119.5 (14)

Symmetry code: (i) $-x, -y + 1, -z$.

H atoms attached to C atoms were placed in geometrically idealized positions and refined riding on their carrier atoms, with aromatic, methyl and methylene C—H distances of 0.95, 0.98 and 0.99 Å, respectively, and with $U_{iso}(H) = 1.5U_{eq}(C)$ for methyl H atoms and $U_{iso}(H) = 1.2U_{eq}(C)$ for the other H atoms. Atom H1 (attached to N2) was located in a difference Fourier density map and refined freely to give N—H distances of 0.85 (3) and 0.906 (18) Å in (I) and (II), respectively.

For both compounds, data collection: *APEX2* (Bruker, 2006); cell refinement: *SAINT* (Bruker, 2006); data reduction: *SAINT*; program(s) used to solve structure: *SHELXS97* (Sheldrick, 2008); program(s) used to refine structure: *SHELXL97* (Sheldrick, 2008); molecular graphics: *SHELXTL* (Sheldrick, 2008); software used to prepare material for publication: *SHELXTL*.

References

Anderson, H. L., Wylie, A. P. & Prout, K. (1998). *J. Chem. Soc. Perkin Trans. 1*, pp. 1607–1611.
Beletskaya, I., Tyurin, V. S., Tsivadze, A. Y., Guilard, R. & Stern, C. (2009). *Chem. Rev.* **109**, 1659–1713.
Bruker (2006). *APEX2* and *SAINT*. Bruker AXS Inc., Madison, Wisconsin, USA.
Doerksen, R. J. & Thakkar, A. J. (1999). *J. Phys. Chem. A*, **103**, 10009–10014.
Drain, C. M., Varotto, A. & Radivojevic, I. (2009). *Chem. Rev.* **109**, 1630–1658.
Hori, A., Shinohe, A., Yamasaki, M., Nishibori, E., Aoygi, S. & Sakata, M. (2007). *Angew. Chem. Int. Ed.* **46**, 7617–7620.
Huang, T.-H., Chen, Y.-J., Lo, S.-S., Yen, W.-N., Mai, C.-L., Kuo, M.-C. & Yeh, C.-Y. (2006). *Dalton Trans.* pp. 2207–2213.
Kato, A., Sugiura, K., Miyasaka, H., Tanaka, H., Kawai, T., Sugimoto, M. & Yamashita, M. (2004). *Chem. Lett.* **33**, 578–579.
Kuo, M.-C., Li, L.-A., Yen, W.-N., Lo, S.-S., Lee, C.-W. & Yeh, C.-Y. (2007). *Dalton Trans.* pp. 1433–1439.
Nakamura, Y., Aratani, N. & Osuka, A. (2007). *Chem. Soc. Rev.* **36**, 831–845.
Quiñonero, D., Garay, C., Rotger, C., Frontera, A., Ballester, P., Costa, A. & Deyà, P. M. (2002). *Angew. Chem. Int. Ed.* **41**, 3389–3392.
Sheldrick, G. M. (1996). *SADABS*. University of Göttingen, Germany.
Sheldrick, G. M. (2008). *Acta Cryst.* A**64**, 112–122.
Thalladi, V. R., Weiss, H.-C., Blaeser, D., Boese, R., Nangia, A. & Desiraju, G. R. (1998). *J. Am. Chem. Soc.* **120**, 8702–8710.
Williams, J. H. (1993). *Acc. Chem. Res.* **26**, 593–598.